Sunlight activated ultra-stable long persistent luminescence glass ceramic for outdoor information display

Jingtao ZHAO[a,b], Lei LEI[a,*], Renguang YE[a], Junjie ZHANG[a], Xianghua ZHANG[b], Shiqing XU[a,*]

[a] Key Laboratory of Rare Earth Optoelectronic Materials and Devices of Zhejiang Province, Institute of Optoelectronic Materials and Devices, China Jiliang University, Hangzhou 310018, People's Republic of China;

[b] Laboratory of Glasses and Ceramics, Univ Rennes, CNRS, ISCR (Institute des Sciences Chimiques de Rennes) UMR CNRS 6226, University of Rennes 1, Rennes 35042, France.

* Corresponding author.

E-mail: leilei@cjlu.edu.cn; shiqingxu@cjlu.edu.cn

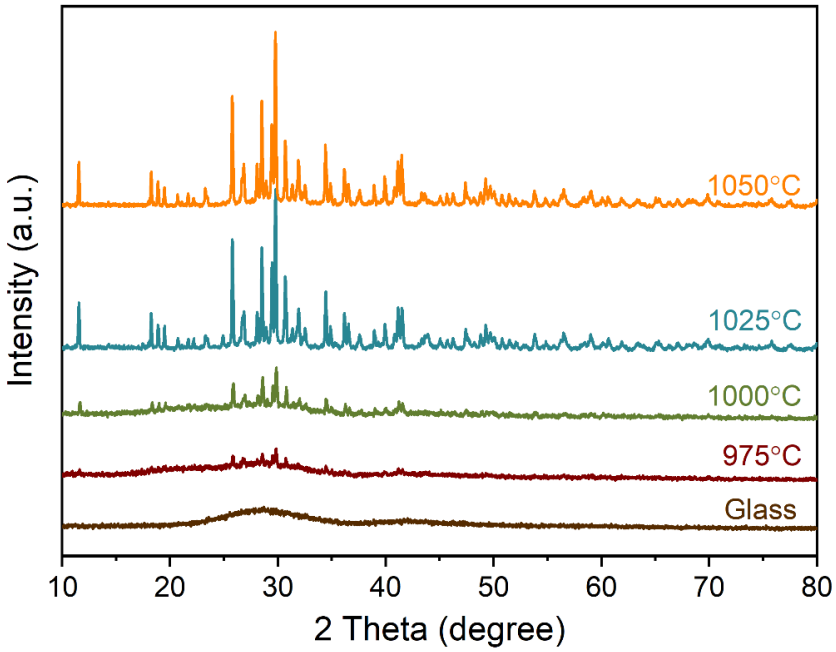

Fig. S1. XRD patterns of the glass and glass ceramics heat treated at different temperature (975, 1000, 1025 and1050 ^{o}C) for 5h. The Glass sample exhibited an amorphous structure, while a crystal phase was precipitated in the glass matrix after heat treatment. The peak intensity was increased with an increase of heat treatment temperature.

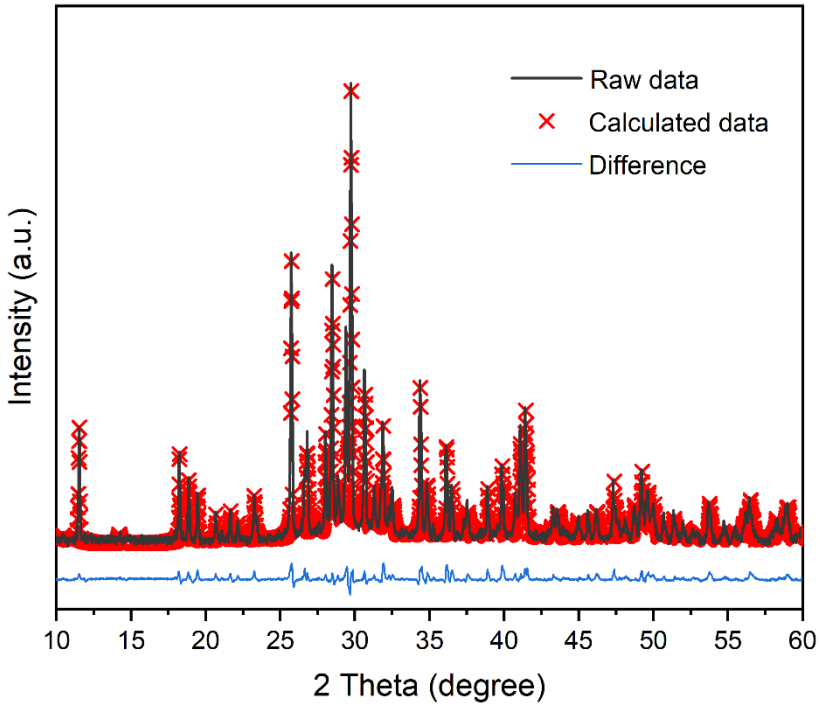

Fig. S2. Experimental and calculated XRD pattern of the Rietveld refinement of GC. The refinement is convergent well with low residual factors of R_p = 6.13%, R_{wp} = 7.36%, and R_{exp} = 3.75%.

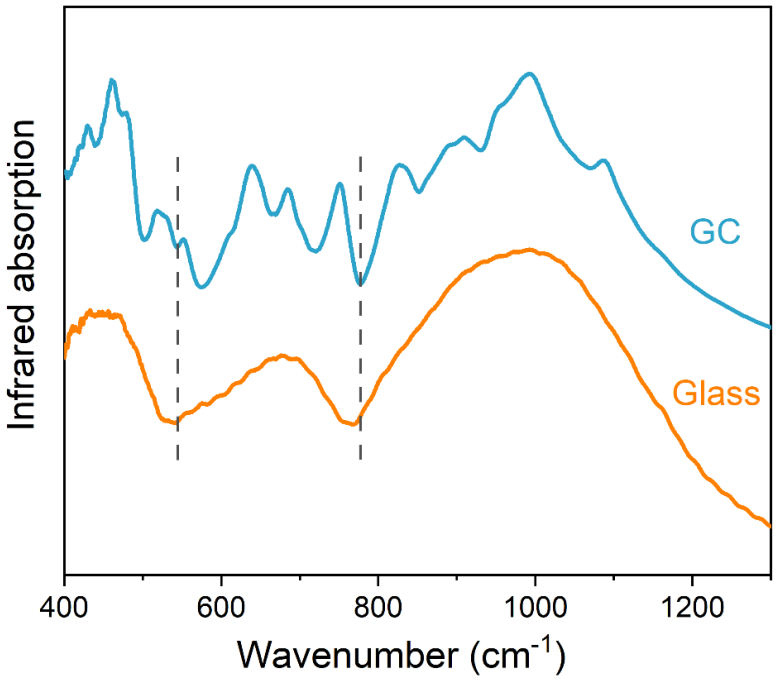

Fig. S3. FTIR spectra of the as-prepared glass and GC. The broad absorption bands located in 400-550 cm^{-1}, 600–800 cm^{-1}, and 800–1200 cm^{-1}, which are corresponding to the bending vibrations of Si–O–Si (Si–O–Al) linkages, stretching vibrations of the Al–O bonds in [AlO_4] tetrahedron and the stretching vibrations of the [SiO_4] tetrahedron, respectively.

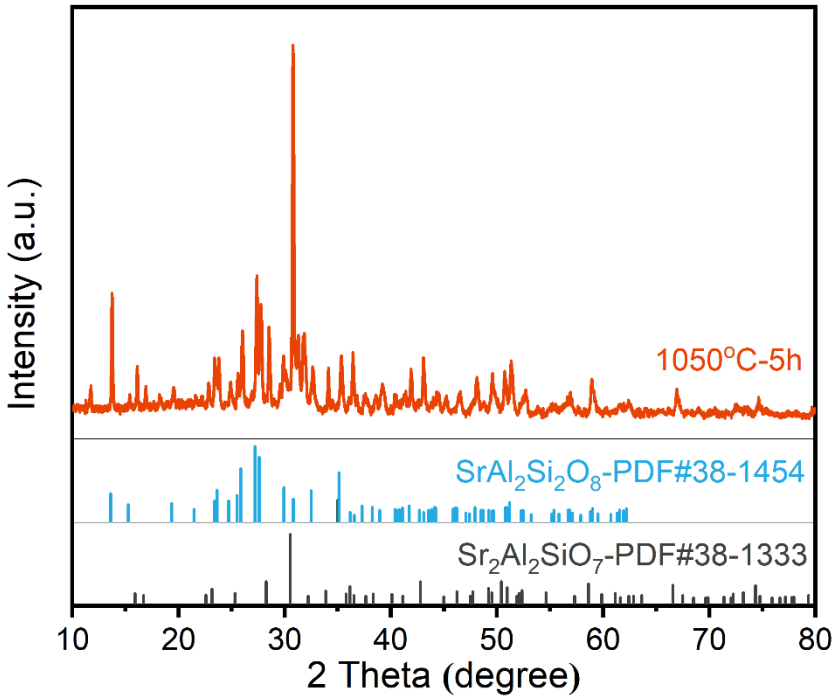

Fig. S4. XRD pattern of the glass ceramic prepared without Si_3N_4 and heated treated at 1050°C for 5h. This product was a mixture of $SrAl_2Si_2O_8$ and $Sr_2Al_2SiO_7$ crystals.

It was reported that Si_3N_4 can be used as nitrogen source to prepare oxynitride phosphors

with excellent luminescence properties (ref: *Nat. Mater.* 2014, **13**: 891-896.; *J. Mater. Chem.* 2012, **22**: 14068-14075.; *Chem. Mater.* 2021, **33**: 7897-7904.). In air or non-nitrogen environment, Si_3N_4 can be decomposed into N_2 and Si at high temperature. Generally, as an important element for the formation of glass, Si is usually introduced by SiO_2, meanwhile, a large amount of oxygen is also generated in the glass network followed by the formation of bridging oxygen and non-bridging oxygen. However, when employing Si_3N_4 as a Si source to prepare glass, Si atoms are preserved in the glass system while the N_2 is volatilized from the glass system. Thus, the ratio of bridging oxygen to non-bridging oxygen will be changed, which further changes the crystallization properties. In our case, the Si_3N_4 promotes the formation of pure hexagonal $Sr_{13}Al_{22}Si_{10}O_{66}$ phase.

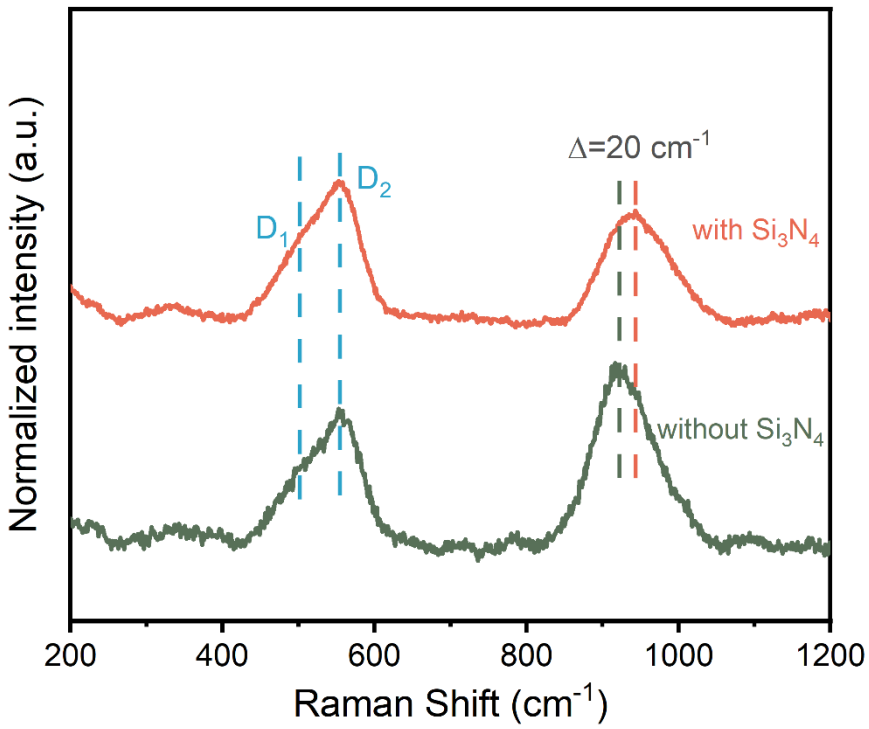

Fig. S5. Raman spectra of the glasses prepared with or without S_3N_4. The Si-O stretching vibration peak (around 920 cm^{-1}) shifted toward high frequency by 20 cm^{-1} after the addition of Si_3N_4.

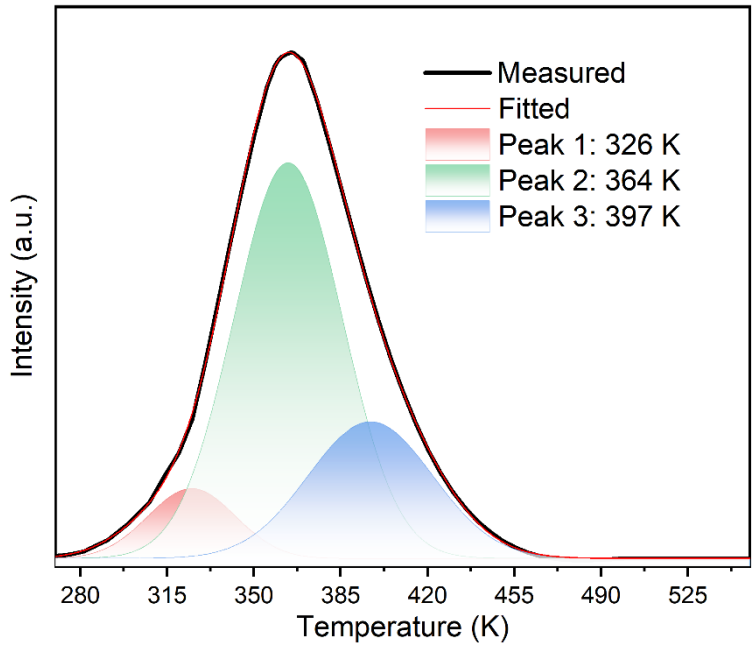

Fig. S6. TL spectra of the GC in the range of 270 to 550 K at a heating rate of 5 K/s. It can be well fitted into three bands.

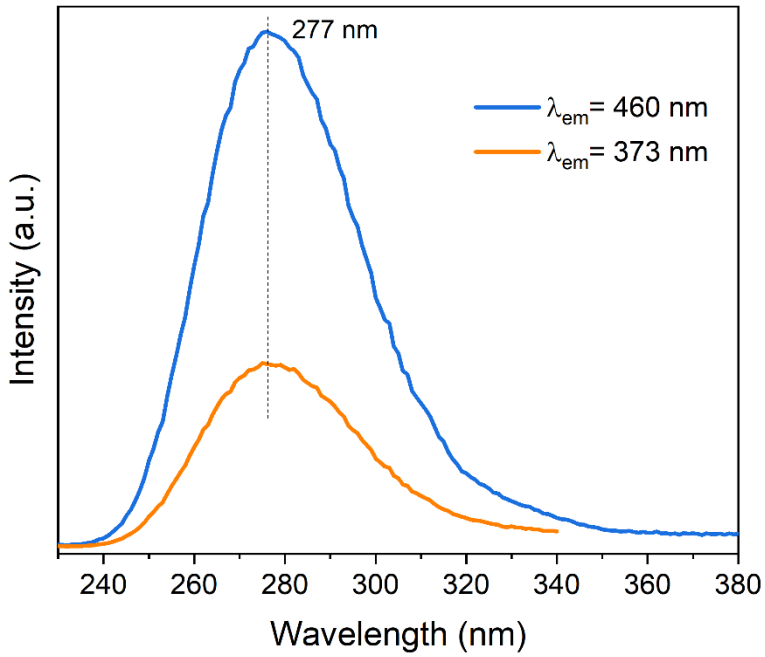

Fig. S7. PLE spectra of the GC monitored at 460 nm and 373 nm. The PLE spectra suggest that the emission bands of 373 nm and 460 nm are corresponding to the same excitation.

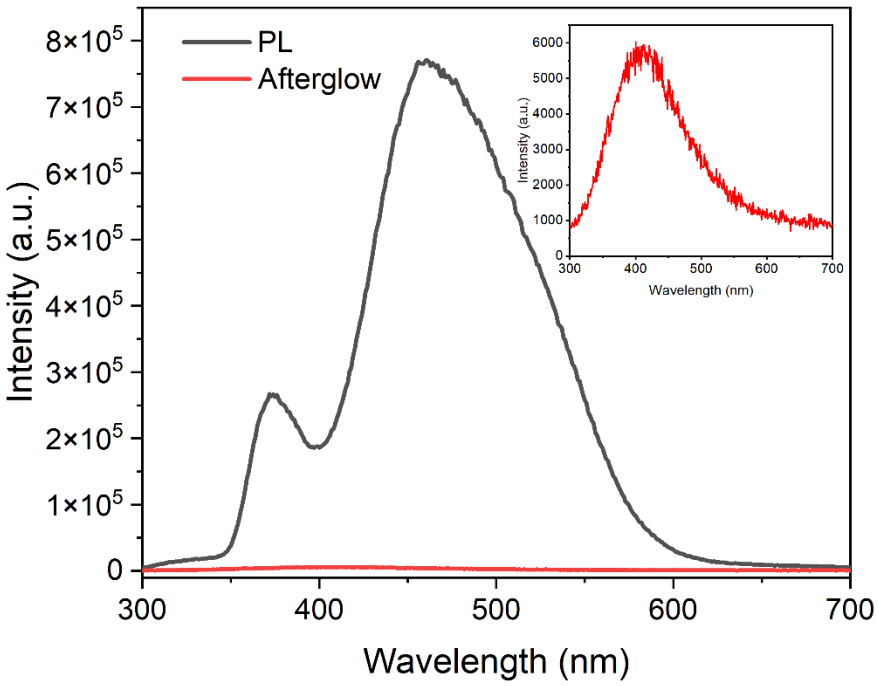

Fig. S8. PL and PeL spectra of the GC. The PeL spectrum was recorded after the cessation of 280 nm light immediately, the delay is about 1s. Inset is the zoom in the spectrum of the GC.

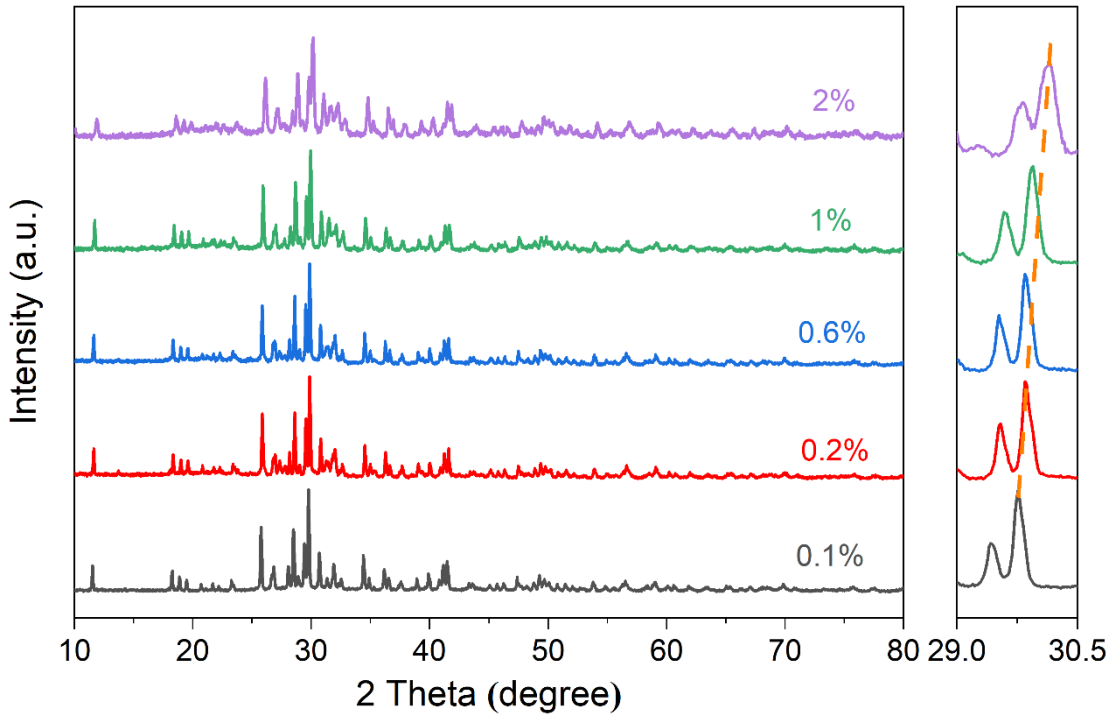

Fig. S9 XRD patterns (left) and the corresponding Zoom in patterns from 29 to 31.5 degrees (right) of the GC:Eu with different Eu doping concentrations. The crystal structure is not changed with tuning the Eu doping concentration, but the peaks shift toward high angels with an increase of Eu doping concentration.

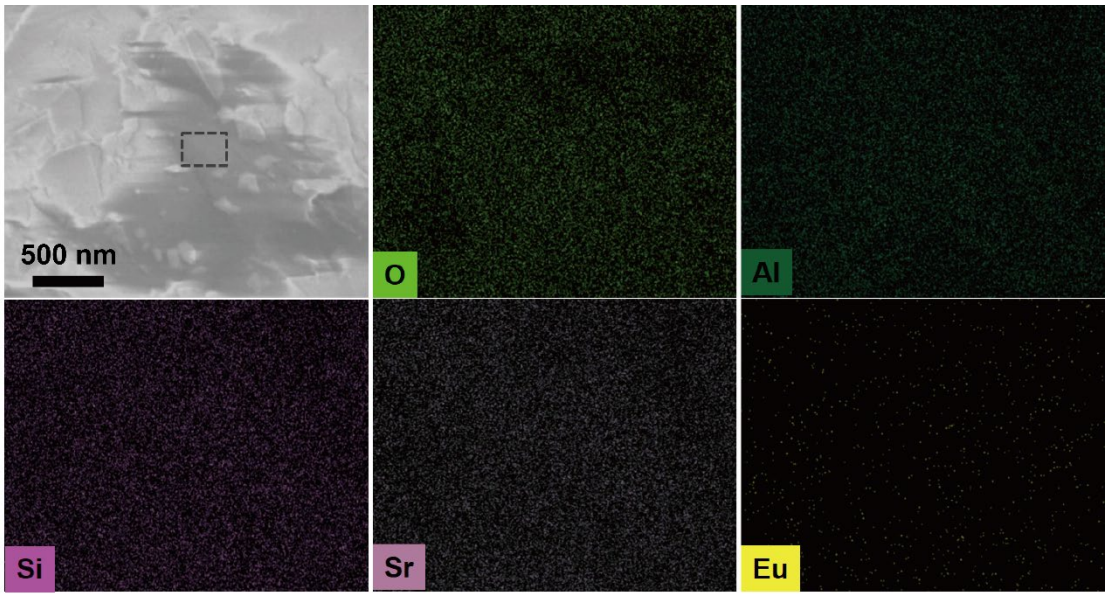

Fig. S10. SEM image and the corresponding EDX element mapping results of the GC:Eu. All the recorded elements were uniformly distributed in the GC:Eu sample.

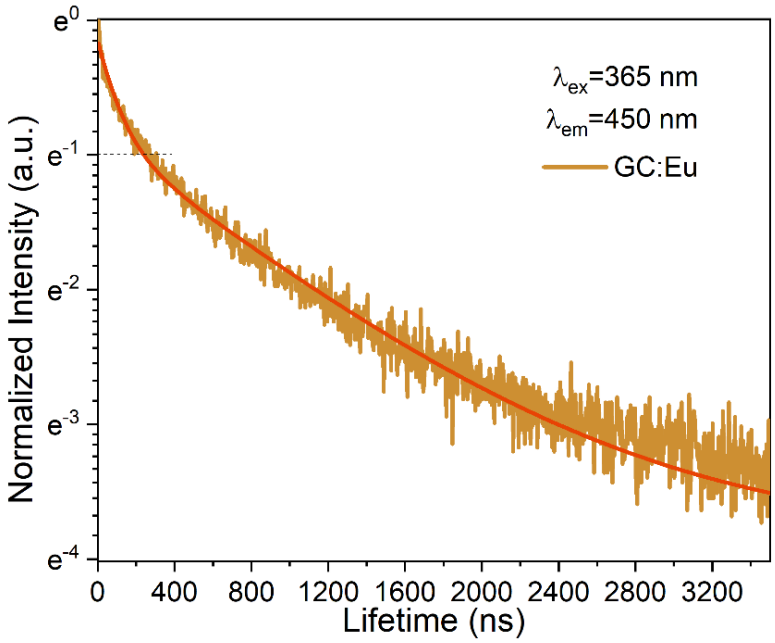

Fig. S11. Luminescence decay curve of the GC:Eu (450 nm). A pulsed 365 nm Nano LED was used as excited source. The calculated lifetime of Eu^{2+} ($4f^{6}5d^{1}\rightarrow 4f^{7}$) is about 241 ns.

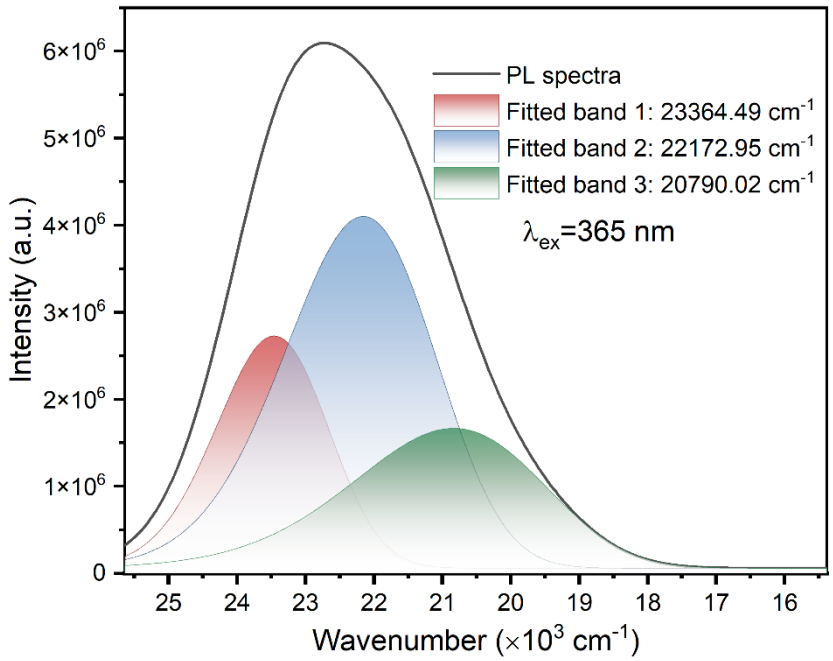

Fig. S12. Fitted PL spectra of the GC:Eu under the excitation of 365 nm light. The PL spectra can be fitted into three emission bands, 23364.49 cm^{-1}, 22172.95 cm^{-1}, and 20790.02 cm^{-1}.

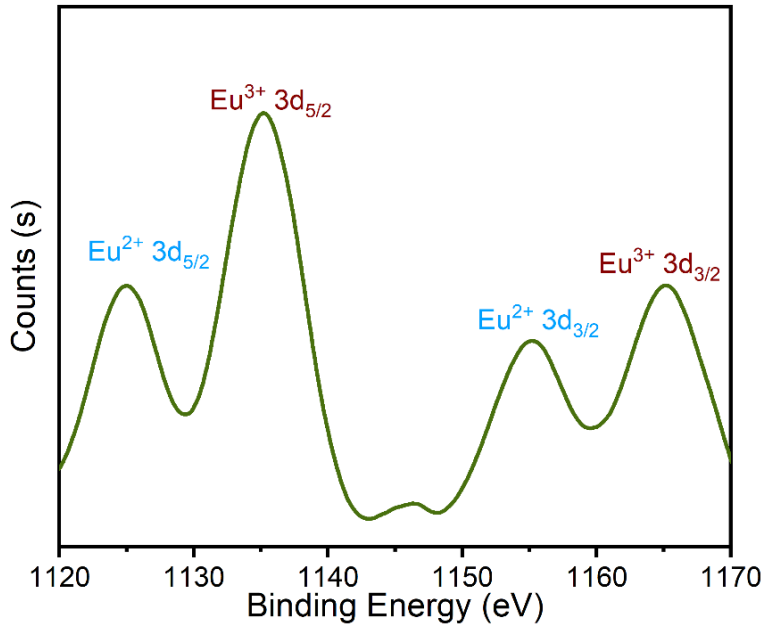

Fig S13. XPS spectrum of the Eu $3d_{5/2}$ and Eu $3d_{3/2}$ in the 0.2 mol% Eu doped GC:Eu sample. The calculated doping contents of Eu^{2+} and Eu^{3+} were about 0.064 and 0.136 mol%, respectively.

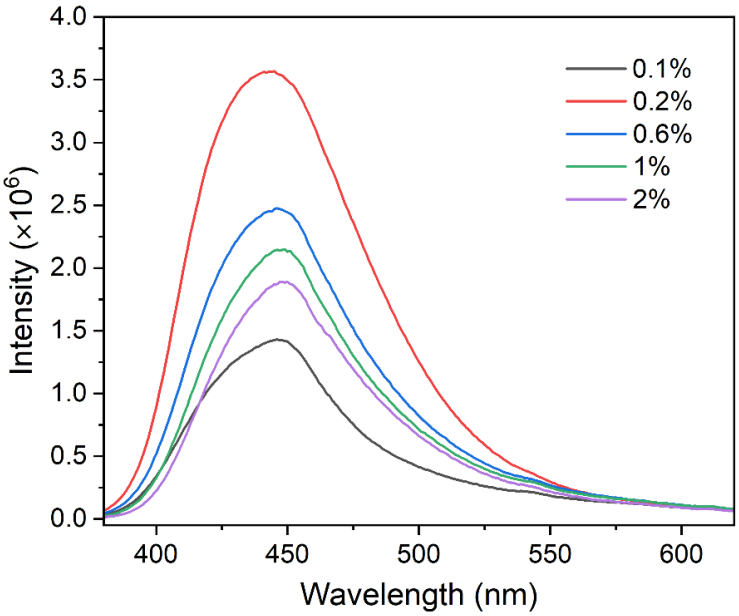

Fig. 14. PeL spectra of the GC:Eu doped with different Eu concentrations (irradiated by 365 nm light for 5min). The GC sample doped with 0.2 mol% Eu exhibited the strongest initial PeL intensity after ceasing the UV light.

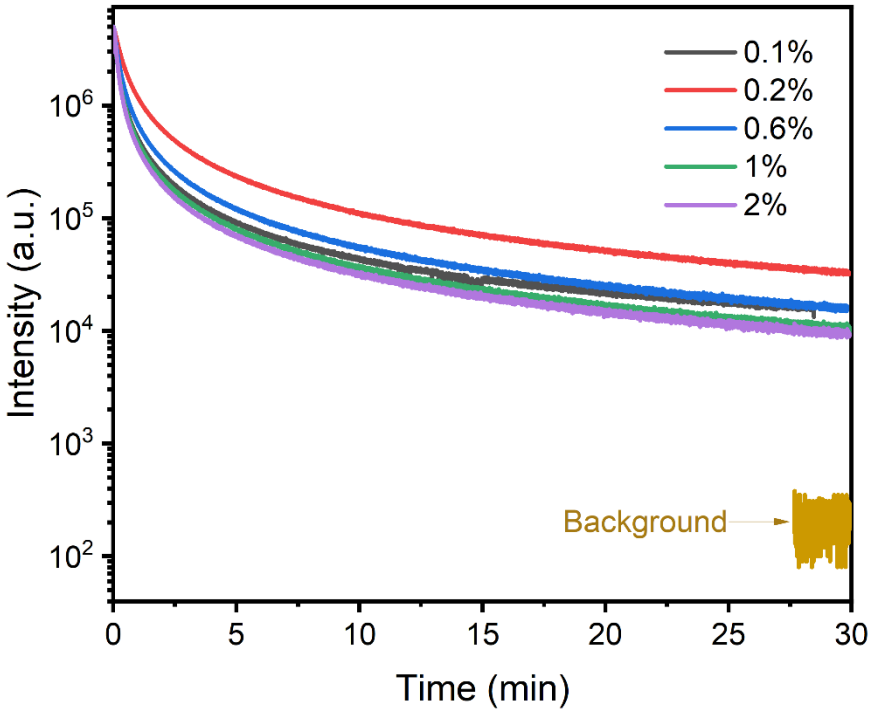

Fig. S15. Normalized PeL intensity decay curves of the GC:Eu doped with different Eu concentrations (irradiated by 365 nm light for 5min). The GC sample doped with 0.2 mol% Eu exhibited the strongest PeL intensity at 30 min after ceasing the UV light.

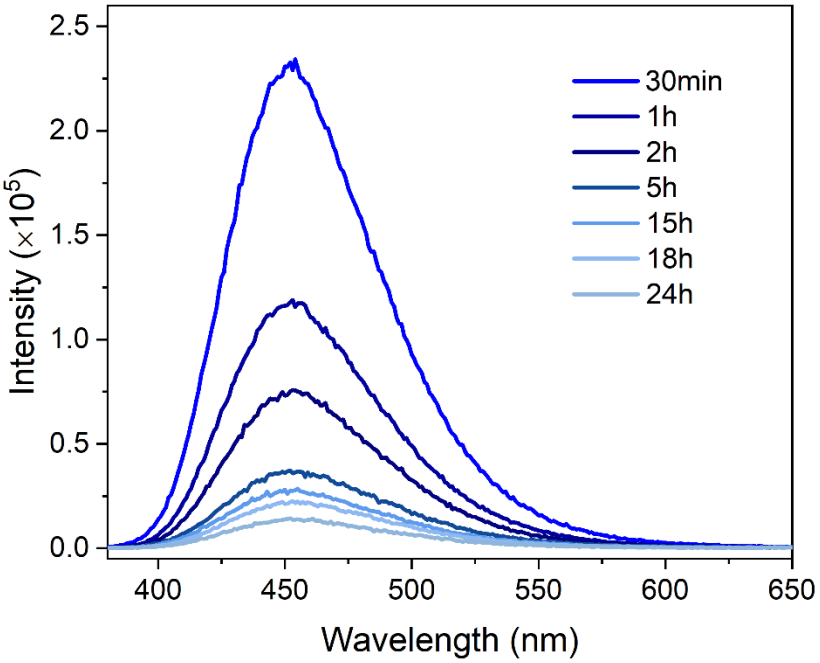

Fig. S16. PeL spectra of the GC:Eu sample at different time (irradiated by 365 nm light for 5min). The PeL intensity decreases gradually over time.

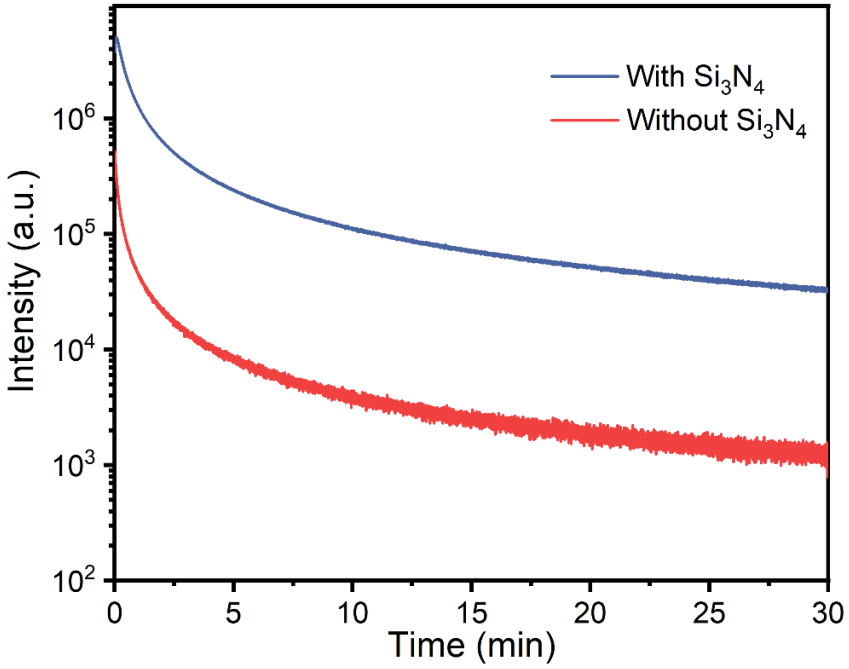

Fig. S17. PeL intensity decay curves of the GC prepared with or without Si_3N_4 (irradiated by 365 nm light for 5min). After the addition of Si_3N_4, the final product exhibits stronger PeL intensity and slow decay rate.

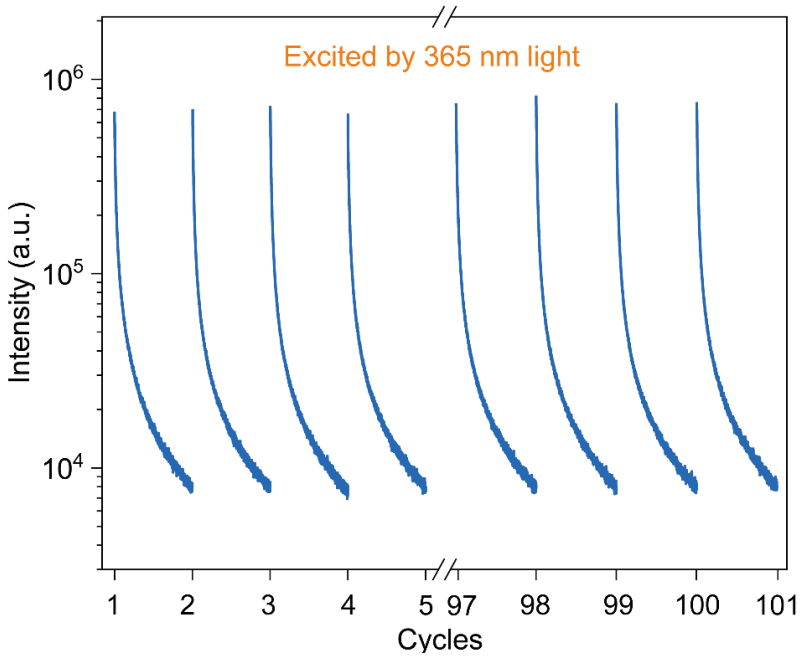

Fig. S18. Repeated PeL decay curves of the GC:Eu after irradiated by 365 nm light for 3 min (each decay time is 30 min). After 100 cycles measurement, the PeL properties such as initial PeL intensity and decay rate were almost remain unchanged.

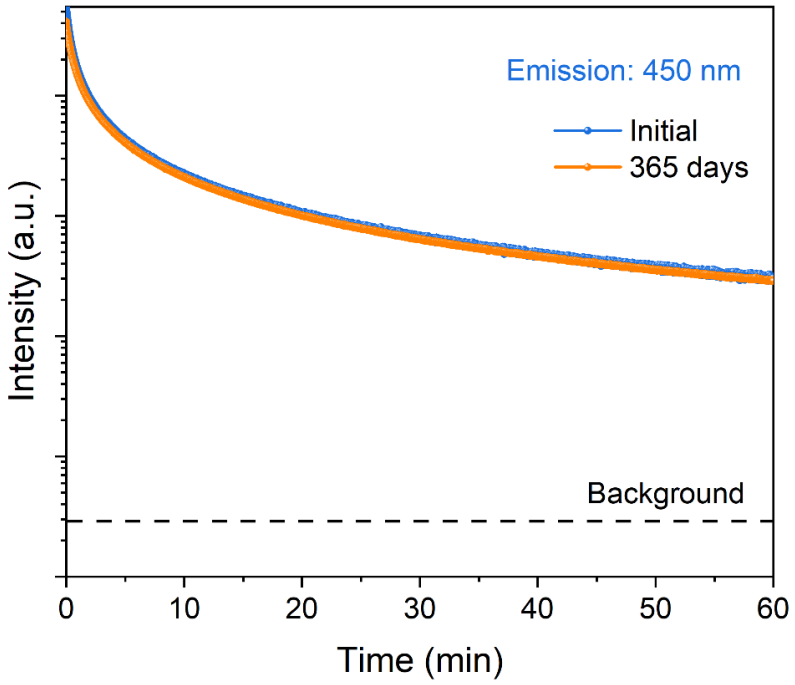

Fig. S19. PeL intensity decay curves of the GC:Eu (bulk) before and after storing in water for 365 days (irradiated by 365 nm light for 5 min). The PeL properties the PeL properties such as initial PeL intensity and decay rate of GC:Eu sample were not changed after storing in water for 365 days.

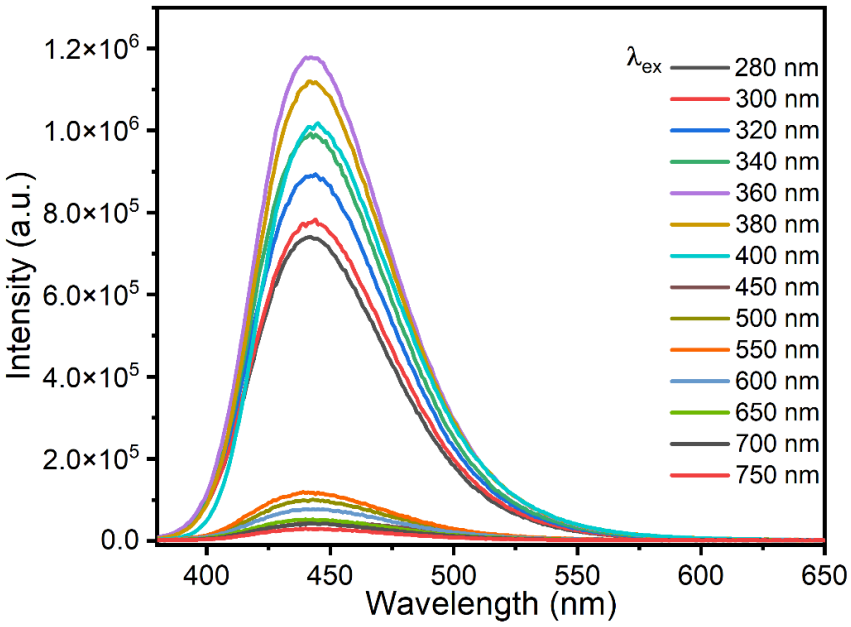

Fig S20. PeL spectra of the GC:Eu irradiated by different excitation wavelengths for 5min. Compared with the irradiation wavelengths in the visible range (450 nm to 750 nm), the GC:Eu sample exhibits brighter PeL under UV (280 nm to 400 nm) irradiation.

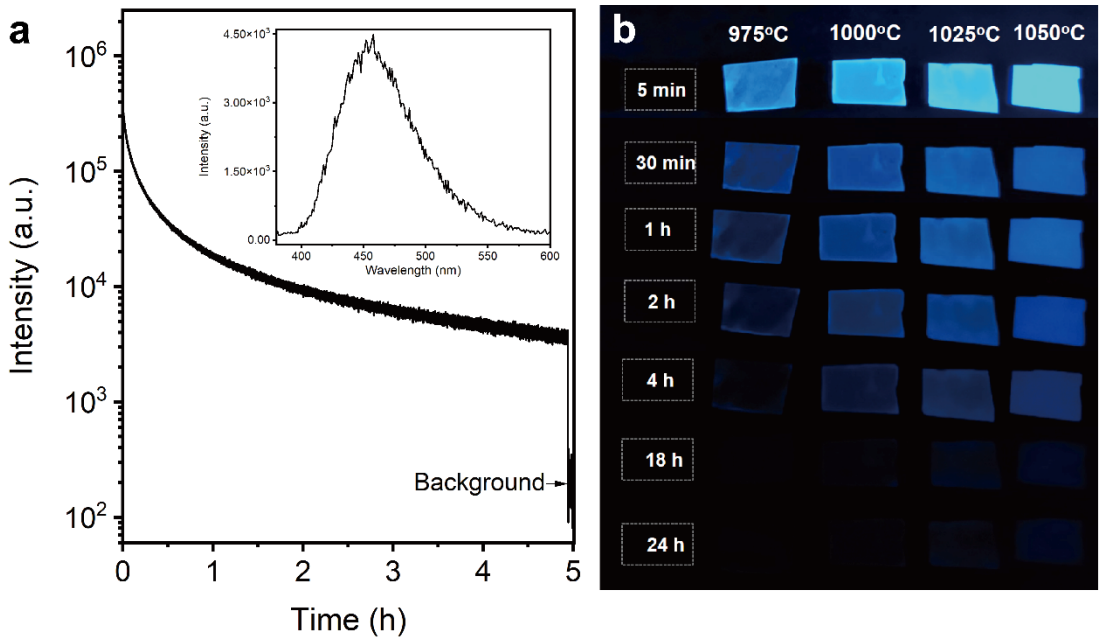

Fig S21. **a** PeL decay curve of the GC:Eu (irradiated by sunlight for 15 min) (inset is the persistent luminescence spectrum after 24 h). **b** Persistent luminescence photographs for the GC:Eu heat treated at different temperatures. The sunlight was used on 25/08/2020 (13:00, Sunny). The bright PeL was clearly observed after exposed to sunlight for 15 minutes.

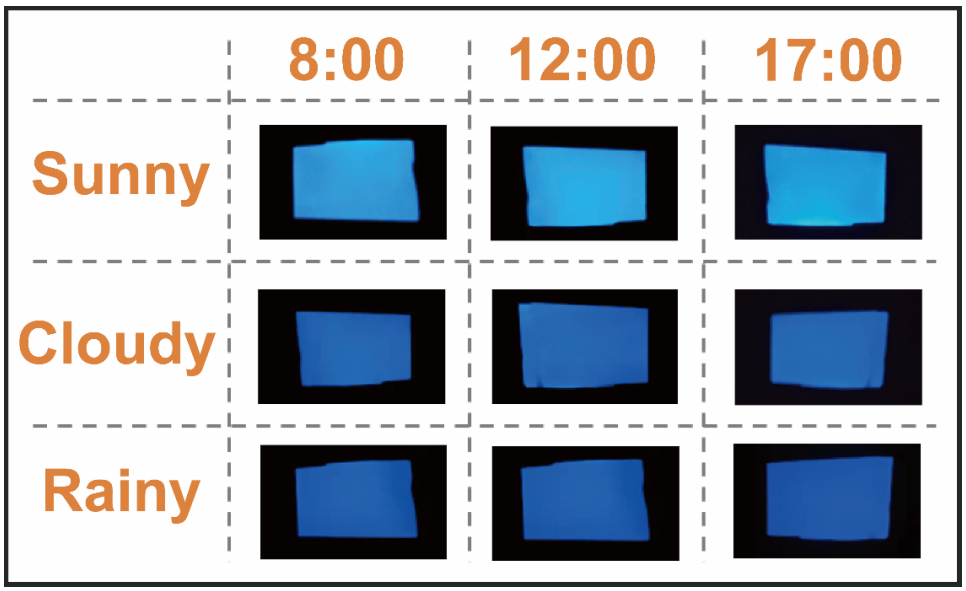

Fig. S22 PeL photographs of the GC:Eu charged by sunlight for 5 min under different weather conditions, Sunny (13/12/2021), Cloudy (14/12/2021) and Rainy (12/12/2021). Regardless of weather conditions (sunny, cloudy, or rainy) and time (morning, noon, or afternoon), the GC:Eu sample can be charged effectively.

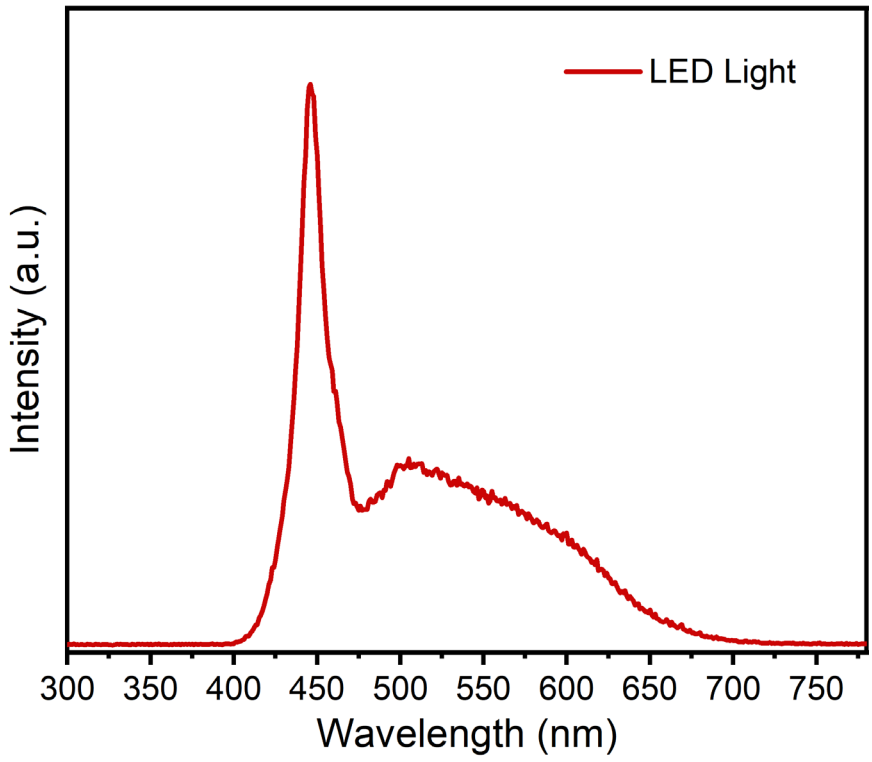

Fig. S23. Recorded spectrum of the used white LED. Its spectrum covers the whole visible region and can be used to stimulate the GC:Eu sample to produce strong PeL.

Fig. S24. PeL photographs of the GC:Eu after 24 h at room temperature (left) and heated at 150 ^{o}C (right). The PeL intensity after 24 h is quite weak, but it can be brightening again through heating, indicating that the deep traps with a slow electron releasing rate can capture many electrons as well.

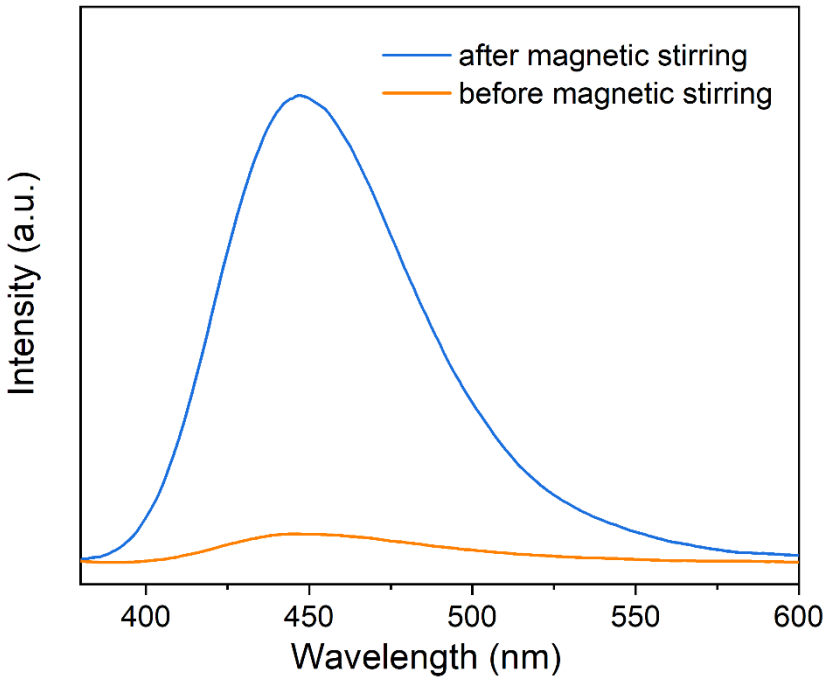

Fig. S25. PeL spectra of the 0.1 mol% Eu_2O_3 doped GC sample before and after magnetically stirring. The sample was excited by 365 nm light for 5min, the spectra (magnetic stirring or not) were recorded after a duration of 5h.

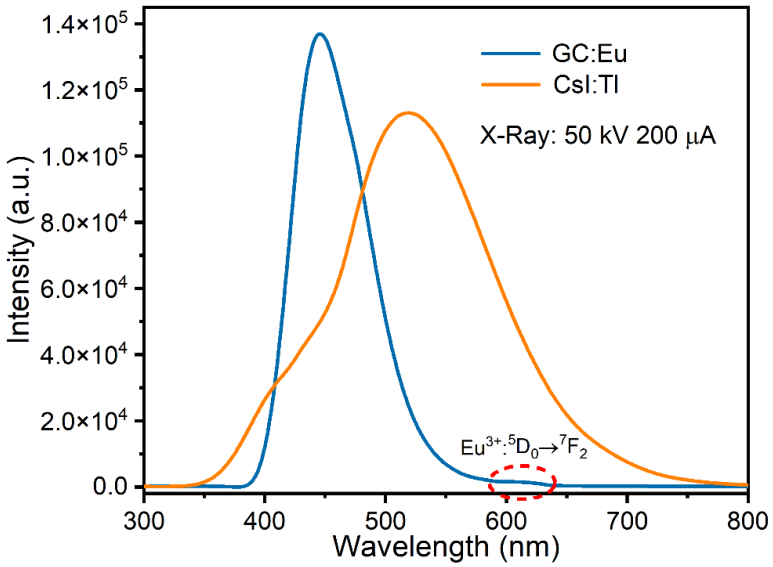

Fig. S26. X-ray excited luminescence spectra of the GC:Eu and commercial CsI:Tl single crystal. To compare the X-ray excited luminescence of GC:Eu and CsI:Tl crystal, the sample thickness (2 mm) and the measurement conditions (50 KV, 200 μA) were the same.

The 4f-4f transition of the Eu^{3+} is spin-forbidden based on the parity selection rule. Different from Eu^{3+}, the 4f-5d transition in Eu^{2+} is parity allowed transition, thus, the strong PL intensity of Eu^{2+} is recorded even with low doping concentration. Under high energy X-ray irradiation, the Eu^{3+}:$^5D_0 \rightarrow {}^7F_2$ emission intensity was much weaker than that of Eu^{2+}. Thus, the PL and PeL emissions from Eu^{3+} can be ignored in our case.

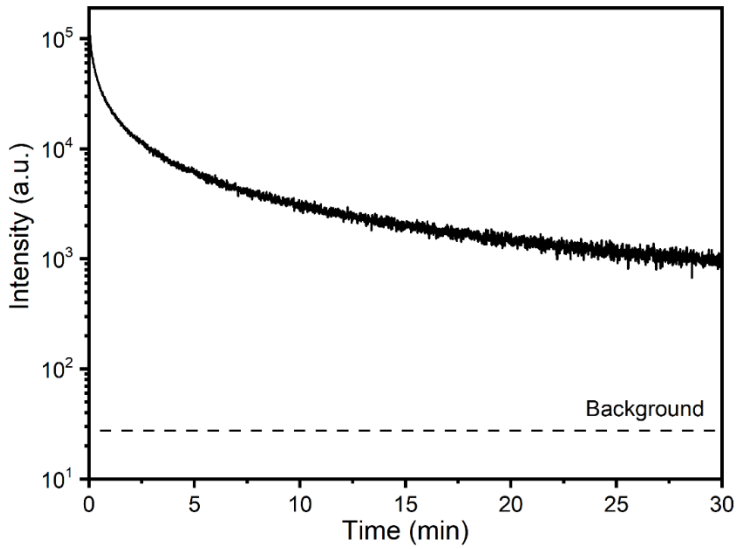

Fig. S27. Persistent luminescence intensity decay curve of the GC:Eu (irradiated by X-rays for 5min). After 30 min, the PeL intensity was remain much stronger than that of background.